


# Unconventional Pairing Induced Anomalous Transverse Shift in Andreev Reflection

Zhi-Ming Yu,<sup>1</sup> Ying Liu,<sup>1</sup> Yugui Yao,<sup>2</sup> and Shengyuan A. Yang<sup>1</sup>

<sup>1</sup>Research Laboratory for Quantum Materials, Singapore University of Technology and Design, Singapore 487372, Singapore

<sup>2</sup>Beijing Key Laboratory of Nanophotonics and Ultrafine Optoelectronic Systems, School of Physics, Beijing Institute of Technology, Beijing 100081, China

 (Received 19 September 2017; revised manuscript received 12 March 2018; published 25 October 2018)

Superconductors with unconventional pairings have been a fascinating subject of research, for which a central issue is to explore effects that can be used to characterize the pairing. The process of Andreev reflection—the reflection of an electron as a hole at a normal-metal–superconductor interface—offers a basic mechanism to probe the pairing. Here we predict that in Andreev reflection from unconventional superconductors, the reflected hole acquires an anomalous spatial shift normal to the plane of incidence, arising from the unconventional pairing. The transverse shift is sensitive to the superconducting gap structure, exhibiting characteristic features for each pairing type, and can be detected as voltage signals. Our work not only unveils a fundamentally new effect with a novel underlying mechanism, but also suggests a possible new technique capable of probing the structure of unconventional pairings.

DOI: [10.1103/PhysRevLett.121.176602](https://doi.org/10.1103/PhysRevLett.121.176602)

Interface scattering—the scattering at an interface between different media—is ubiquitous for all kinds of particles and waves. It offers a basic means to probe material properties and is of fundamental importance for controlling carrier transport. Nontrivial effects can happen during interface scattering. In geometric optics, it is known that a circularly-polarized light beam undergoes a transverse shift, normal to its plane of incidence when reflected at an optical interface, called the Imbert-Fedorov (IF) shift [1–6]. Recently, an analogous effect has been discovered for electronic systems, showing that transverse shifts also appear for electrons in so-called Weyl semimetals [7–10]. In both cases, the spin-orbit coupling (SOC) plays the key role. The light helicity, corresponding to the photonic spin state, intrinsically couples with the light propagation in the Maxwell equation [11], and the low-energy electrons in Weyl semimetals also possess a strong SOC described by the Weyl equation [12,13]. Upon scattering, any change in the particle spin would require a change in the orbital motion due to SOC, resulting in the anomalous spatial shift.

There is an intriguing and unique scattering process occurring at the normal-metal–superconductor (NS) interface—the Andreev reflection, in which an incident electron from the normal metal is reflected back as a hole, accompanied by the transfer of a Cooper pair into the superconductor [14,15]. Most recently, we find that the transverse shift can also exist in the Andreev reflection, if the interface is formed by a spin-orbit-coupled metal and a conventional *s*-wave superconductor [16]. It is important to note that the essential ingredient there is still the assumed strong SOC of the scattered carrier—the shift vanishes when the SOC is negligible, whereas the superconductivity

only plays a *passive* role as a channel for electron-hole conversion.

Unconventional pairing brings new physics into the picture. By breaking more symmetries than the U(1) gauge symmetry, unconventional pair potentials necessarily have a strong wave vector dependence [17]. Surprisingly, we find that in an Andreev reflection from an unconventional superconductor, a sizable transverse shift exists even in the *absence* of the SOC, resulting solely from the unconventional pair potential. We show that the unconventional pairing provides an *effective* coupling between the orbital motion and the pseudospin of the electron-hole (Nambu) space, which underlies this exotic effect. Remarkably, the value of the shift is sensitive to the structure of the pair potential, and it manifests characteristic features for each pairing type, as summarized in Table I. The effect can be detected through electric measurement, providing a promising new technique for probing the structure of unconventional pairings.

TABLE I. Features of the transverse shift for typical unconventional pair potentials. “No. of SZ” stands for the number of suppressed zones when the rotation angle  $\alpha$  varies from 0 to  $2\pi$ .

	Pair potential	Expression		Period in $\alpha$	Vanish for $\varepsilon >  \Delta(\alpha) $	No. of SZ
		$\ell_T^e$	$\ell_T^h$			
Chiral	$\Delta_0 e^{i\chi\phi_k}$	0	$\frac{\chi}{k_F^y \sin \gamma}$	...	No	0
$p_x$	$\Delta_0 \cos \phi_k$			$\pi$		2
$p_y$	$\Delta_0 \sin \phi_k$			$\pi$	Yes	2
$d_{x^2-y^2}$	$\Delta_0 \cos 2\phi_k$	$\ell_T^e \approx \ell_T^h$		$\pi/2$		4
$d_{xy}$	$\Delta_0 \sin 2\phi_k$			$\pi/2$		4

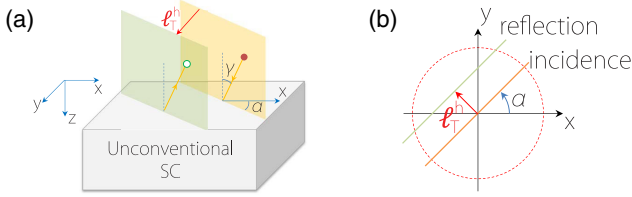


FIG. 1. (a) Schematic of the NS junction setup. In the Andreev reflection, the reflection plane (green colored) is shifted by distance  $\ell_T^h$  from the incident plane (orange colored) along its normal direction ( $\hat{n}$ ), due to an unconventional pairing in  $S$ . Here,  $\hat{n}$  is specified to be along  $\hat{k} \times \hat{z}$  with  $\hat{k}$  the incident direction. (b) Top view of the  $x$ - $y$  plane in (a). For certain pairings, there may also be a finite shift  $\ell_T^e$  for normally-reflected electrons (not shown here).

*Model.*—Since our goal is to demonstrate the existence of the finite transverse shift, we take a simplest model for a three-dimensional NS junction with a flat interface in the clean limit. In this Letter, we focus on the case where the interface is perpendicular to the principle rotation axis (along the  $z$  direction) of the superconductor [Fig. 1(b)]. Configurations with other interface orientations can be similarly studied. To highlight the role of unconventional pairing, we neglect SOC in the model. Then, for each pairing considered in Table I, the essential physics of scattering at the NS interface (located at  $z = 0$ ) can be captured by the Bogoliubov–de Gennes (BdG) equation [15,18,19] in the following reduced form

$$\begin{bmatrix} H_0 - E_F + V(z) & \Delta(z) \\ \Delta^*(z) & E_F - H_0 - V(z) \end{bmatrix} \psi = \epsilon \psi. \quad (1)$$

Here,  $\psi$  is the two-component spinor wave function in the Nambu space (the real-spin labels are suppressed),  $E_F$  is the Fermi energy, and  $V(z) = U\Theta(z) + h\delta(z)$  with  $U$  the band bottom shift,  $h$  the interface barrier potential, and  $\Theta$  the Heaviside step function. We take the single-particle Hamiltonian  $H_0 = -[1/(2m)]\nabla^2$  for the normal-metal ( $N$ ) side ( $z < 0$ ), and  $H_0 = -[1/(2m_{\parallel})](\partial_x^2 + \partial_y^2) - [1/(2m_z)]\partial_z^2$  for the superconductor ( $S$ ) side ( $z > 0$ ). The difference in the effective masses  $m_{\parallel}$  and  $m_z$  describes the possible uniaxial anisotropy in  $S$ . For certain layered superconductors (like cuprates), the Fermi surface is highly anisotropic and may take a cylinderlike shape in the normal state. Such a case can be described using a lattice model, and we find that the essential features of our results remain the same [20]. For concrete calculations, we take the usual step function model for the pair potential  $\Delta(z) = \Delta\Theta(z)$  [18,34]. It is a good approximation to the full self-consistent solution for the BdG equation near an interface [35–37], and as we show below, for certain cases with an emergent symmetry, the transverse shift does not actually depend on the detailed  $z$  variation of  $\Delta(z)$ . We consider the weak coupling limit with  $E_F - U \gg |\Delta|$ ,  $\epsilon$  in the  $S$  region,

so that the wave vector for  $\Delta$ 's  $k$ -dependence is fixed on the (normal-state) Fermi surface of  $S$ , and  $\Delta$  only depends on the direction of the wave vector  $\mathbf{k}$  [38].

*Intuitive picture & symmetry argument.*—The spatial shift is defined for a confined electron beam undergoing a reflection at the interface. The incident geometry is characterized by two angles,  $\gamma$  and  $\alpha$ , as illustrated in Fig. 1. The beam is usually modeled by a wave packet  $\Psi$  [7,16,21], which is assumed to be confined in both real and momentum spaces. The detailed form of  $\Psi$  does not concern us for now.

Let us first consider the case when  $\Delta$  is of the chiral  $p$ -wave pairing, with  $\Delta = \Delta_0 e^{i\chi\phi_k}$ , because it offers an intuitive understanding of the physical picture. Here,  $\chi = \pm 1$  denotes the chirality,  $(\theta_k, \phi_k)$  are the spherical angles of  $\mathbf{k}$ , and  $\Delta_0$  is assumed to be independent of  $\phi_k$  but may still depend on  $\theta_k$ . A key observation is that the BdG equation possesses an emergent symmetry:

$$[\hat{\mathcal{H}}_{\text{BdG}}, \hat{\mathcal{J}}_z] = 0, \quad (2)$$

where  $\hat{\mathcal{H}}_{\text{BdG}}$  is the BdG Hamiltonian in Eq. (1), with  $\Delta$  taking the chiral  $p$ -wave form, and

$$\hat{\mathcal{J}}_z = (\hat{\mathbf{r}} \times \hat{\mathbf{k}}) - \frac{1}{2} \chi \hat{\tau}_z \quad (3)$$

resembles an effective angular momentum operator with  $\hat{\tau}_z$  the Pauli matrix corresponding to the Nambu pseudospin-1/2. Consequently, the expectation value  $J_z = \langle \Psi | \hat{\mathcal{J}}_z | \Psi \rangle$  evaluated for the beam must conserve during scattering. For electrons and holes, the expectation values of the Nambu pseudospin are the opposite:  $\langle \hat{\tau}_z \rangle_{e/h} = \pm 1$ . Because the pseudospin flips in the Andreev reflection, the conservation of  $J_z$  must dictate a transverse shift  $\ell_T^h$  to compensate this change (see Fig. 1), leading to

$$\ell_T^h = -\frac{\chi}{2k_{\parallel}} (\langle \hat{\tau}_z \rangle_h - \langle \hat{\tau}_z \rangle_e) = \frac{\chi}{k_{\parallel}}, \quad (4)$$

where  $k_{\parallel} = k_F^N \sin \gamma$ ,  $k_F^N$  is the Fermi wave vector in  $N$ , and  $\gamma$  is the incident angle.

This remarkable result demonstrates several points. First, the physical picture becomes clear: the shift here is entirely due to the unconventional pairing, which plays the role of an *effective* SOC that couples  $k$  and  $\tau$ . However, the spin here is not the real spin but the Nambu pseudospin, which is *intrinsic* and *unique* for superconductors. The change in pseudospin during the Andreev reflection then naturally results in the shift in real space. Second, resulting from a symmetry argument, Eq. (4) is quite general: as long as the symmetry is preserved, factors like the variation of  $\Delta(z)$ , the excitation energy, or the interfacial barrier will not affect  $\ell_T^h$ . Third, the result of Eq. (4) also applies for chiral pairings with higher orbital moments ( $|\chi| > 1$ ), such as  $d + id$  or  $f + if$  pairings. Finally, the shift becomes

pronounced when  $k_F^N$  (or  $\gamma$ ) is small, when the  $N$  side is of a doped semiconductor or semimetal with small Fermi surfaces, a feature similar to analogous effects discussed before [7,8].

*Scattering approach.*—For general cases without a conserved  $\mathcal{J}_z$ , the shift can be obtained via the quantum scattering approach [7,16,21], which has been the standard in studying the shift in optical and electronic contexts. In this approach,  $\Psi$  is expanded using the scattering eigenstates of the system. For example, the incident beam  $\Psi_k^{e+}(\mathbf{r}) = \int d\mathbf{k}' w(\mathbf{k}' - \mathbf{k}) \psi_k^{e+}(\mathbf{r})$ , where  $w$  is the profile of the beam peaked at  $\mathbf{k}$ , and  $\psi^{e+}$  is the incident electron eigenstate. At the interface, each partial wave  $\psi^{e+}$  gets scattered. Particularly, for the Andreev reflection,  $\psi^{e+}$  is reflected as  $\psi^{h-}$  with an amplitude  $r_h$ ; hence the reflected hole beam is given by  $\Psi_k^{h-}(\mathbf{r}) = \int d\mathbf{k}' w(\mathbf{k}' - \mathbf{k}) r_h(\mathbf{k}') \psi_k^{h-}(\mathbf{r})$ . The spatial shift is obtained by comparing the center positions of the two beams at the interface. One easily finds that the shift here takes a simple form

$$\delta \ell_i^h = -\frac{\partial}{\partial k_i} \arg(r_h)|_{k_{\parallel}}, \quad (5)$$

where  $i \in \{x, y\}$ ,  $\mathbf{k}_{\parallel}$  is the average transverse wave vector that is conserved in scattering, and  $\arg(r_h)$  is the phase of  $r_h$ . In this approach, the spatial shift appears as a result of the interference between the scattered partial waves. As evident from Eq. (5), it only depends on (the  $k$ -dependence of) the phase of the scattering amplitude, not the magnitude.

We have some additional remarks. (i) There may also exist a shift  $\delta \ell_i^e$  for the normally-reflected electron beam, whose expression takes the same form as Eq. (5) by replacing  $r_h$  with  $r_e$ . (ii) Although the shift does not depend on the magnitudes of  $r_h$  ( $r_e$ ), the intensity of the reflected beam is proportional to  $|r_h|^2$  ( $|r_e|^2$ ). (iii) The shift has both longitudinal (analogous to the Goos-Hänchen shift in optics [39]) and transverse components with reference to the incident plane. In this Letter, we focus on the transverse shift:  $\ell_T^{e(h)} \equiv \delta \ell^{e(h)} \cdot \hat{n}$ , where  $\hat{n}$  is the normal direction of the incident plane, as illustrated in Fig. 1. (iv) The scattering approach is quite general. Unlike the semiclassical approach, which requires the quasiparticle wavelength to be small compared with the perturbation length scale [8], the scattering approach does not suffer from such a constraint, and it applies for sharp interfaces and/or large wavelengths as well [7,16,21].

This approach is applied to study the transverse shift for each type of the pair potentials. The calculation is straightforward, and the key results are tabulated in Table I. For conventional  $s$ -wave pairing, one easily checks that  $\ell_T^e = \ell_T^h = 0$ , consistent with our previous findings [16]. In contrast, the transverse shift can become sizable if the  $S$  side is of an unconventional pairing, and it possesses features tied with the pairing symmetry. We discuss two cases below.

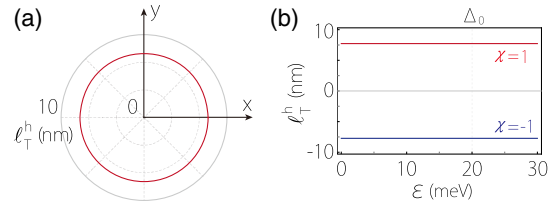


FIG. 2. Transverse shift  $\ell_T^h$  for chiral  $p$ -wave pairing versus (a) the rotation angle  $\alpha$  (here  $\chi = +1$ ), and (b) the excitation energy  $\epsilon$ .  $\ell_T^h$  is independent of  $\epsilon$  and  $\Delta_0$ , and its sign depends on  $\chi$ . Here, we take  $\Delta_0 = 20$  meV,  $\gamma = \pi/12$ ,  $E_F = 0.1$  eV, and  $m = 0.1m_e$ .

*Chiral  $p$ -wave.*—Let us revisit the case for chiral  $p$ -wave pair potential using the scattering approach. Straightforward calculations show that  $\arg(r_h) = -\chi\phi_k$  and  $\arg(r_e)$  is independent of  $k$  [20]. Then, according to Eq. (5),

$$\ell_T^h = \chi/k_{\parallel}, \quad \ell_T^e = 0, \quad (6)$$

which exactly recovers the result we have obtained using the symmetry argument. This result is independent of the incident angles, the excitation energy, and the parameters for the  $S$  side, such as the pairing gap  $\Delta_0$ , except that its sign depends on the chirality  $\chi$  (see Fig. 2).

*$d_{x^2-y^2}$ -wave.*—As another example, we consider the  $d_{x^2-y^2}$ -wave pairing, with  $\Delta = \Delta_0 \cos(2\phi_k)$ . Our calculation gives that [20]

$$\ell_T^h \propto \sin(4\alpha) \Theta(|\Delta_0 \cos 2\alpha| - \epsilon), \quad (7)$$

and  $\ell_T^e \approx \ell_T^h$ . The expression in Eq. (7) highlights the dependence on the rotation angle  $\alpha$  and the excitation energy  $\epsilon$ . The results are plotted in Fig. 3.

From Eq. (7) and Fig. 3, we observe the following key features for the shift. (i)  $\ell_T^{e(h)}$  has a period of  $\pi/2$  in  $\alpha$ , and it flips sign at multiples of  $\pi/4$  [Fig. 3(b)]. (ii)  $\ell_T^{e(h)}$  is sensitive to the gap magnitude. As indicated by the step function in Eq. (7), it is suppressed for excitation energies above the pairing gap at the incident wave vector. (iii) Particularly, due to the nodal structure of the gap, for a fixed excitation energy  $\epsilon$ , there must appear multiple zones in  $\alpha$  where  $\ell_T^{e(h)}$  is suppressed [see Fig. 3(b)]. The center of each suppressed zone coincides with a node. (iv)  $\ell_T^{e(h)}$  is also suppressed when  $k_{\parallel}$  is away from the Fermi surface of the  $S$  side, as indicated in Figs. 3(c) and 3(f), where we compare the results for a closed ellipsoidal Fermi surface and for an open cylinderlike Fermi surface. This can be understood by noticing that the effect of a pair potential diminishes away from the Fermi surface.

The above features of the shifts encode rich information about the unconventional gap structure, including the  $d$ -wave symmetry [Feature (i)], the gap magnitude profile [Feature (ii)], and the node position [Feature (iii)]. Thus, by detecting the effect, one can extract important information

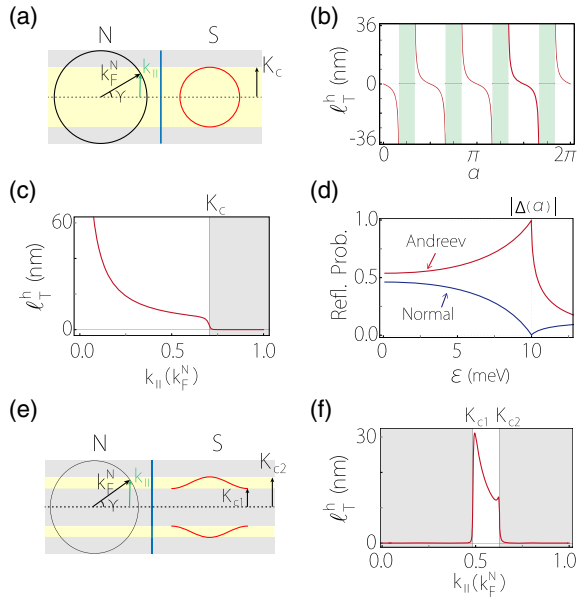


FIG. 3. Results for  $d_{x^2-y^2}$ -wave pairing. (a)–(d) are for the  $S$  side with an ellipsoidal Fermi surface, and (e)–(f) are for the  $S$  with a cylinderlike Fermi surface. (a) Schematic figure showing the Fermi surfaces of  $N$  and  $S$ .  $K_c$  denotes the maximum magnitude of the transverse wave vector on the  $S$  Fermi surface. (b)  $\ell_T^h$  versus  $\alpha$ . The green shaded regions indicate the suppressed zones, in which  $\epsilon > |\Delta(\alpha)|$ . (c)  $\ell_T^h$  versus  $k_{||}$ . Corresponding to (a),  $\ell_T^h$  is suppressed when  $k_{||} > K_c$ , as denoted by the gray shaded region. (d) Reflection probabilities versus  $\epsilon$  for normal and Andreev reflections. (e) illustrates the case when the  $S$  Fermi surface is of an open cylinderlike shape.  $K_{c1}$  and  $K_{c2}$  denote the lower and upper bounds for the transverse wave vector on the  $S$  Fermi surface. For such case, the qualitative features in (b) and (d) remain the same [20]. The main difference is that the shift is now suppressed in regions except for  $K_{c1} < k_{||} < K_{c2}$ , as shown in (f). In (a)–(d), we take  $\Delta_0 = 20$  meV,  $E_F = 0.4$  eV,  $U = 0.2$  eV,  $h = 0.3$  eV · nm, and  $m_{||} = m_z = m = 0.1m_e$ . We set  $\epsilon = 10$  meV and  $\gamma = \pi/12$  in (b);  $\alpha = -\pi/6$  and  $\epsilon = 8$  meV in (c);  $\alpha = \pi/6$  and  $\gamma = \pi/5$  in (d). The parameters for (f) are presented in the Supplemental Material [20].

about the unconventional superconductor. Feature (iv) also offers information on the geometry of the Fermi surface.

**Discussion.**—Here, we have revealed a fundamentally new effect—the anomalous shifts in the Andreev reflection generated by unconventional pairings. Distinct from the previous works [7,8,16], where the shift invariably originates from the SOC in the  $N$  region and vanishes if the SOC is negligible, the shift here is purely from the unconventional pairing in the  $S$  region, and it exists without the need of SOC. Because of this fundamental difference, the shifts here manifest the characteristics of unconventional pairings in  $S$ , such as the highly anisotropic behavior with respect to the incident direction as in Fig. 3(b), which is tied to the anisotropic character of the  $d_{x^2-y^2}$ -pairing; whereas the shifts in Ref. [16] instead reflect the SOC pattern of the  $N$  region.

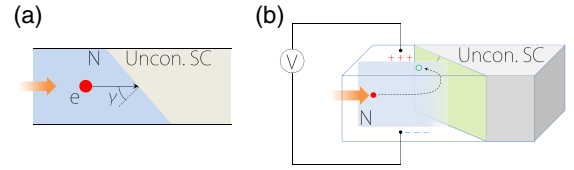


FIG. 4. Schematic (a) top view and (b) side view of a possible NS junction geometry for experimental detection. Electrons are driven to the interface with a finite average incident angle. The effect of transverse shift (in the  $z$  direction) induces a net surface charge accumulation near the junction on the  $N$  side, which can be detected as a voltage difference between top and bottom surfaces. Here, we illustrate the case when Andreev reflections dominate the interface scattering.

To experimentally probe the effect, we suggest a simple NS junction geometry, as illustrated in Fig. 4, in which the electrons are driven towards the interface with a finite average incident angle. The transverse shift then leads to the surface charge accumulation, as indicated in Fig. 4(b), which can be detected as a voltage signal between the top and bottom surfaces. With an order of magnitude estimation [20], we find that the voltage signal can be on the order of mV, readily detectable in the experiment. We also suggest a second setup to amplify the shift through multiple scattering in an SNS structure, which leads to a large anomalous velocity of up to  $10^4$  m/s [20]. With more delicate setups, e.g., by using local gates and collimators similar to those in electron optics [40,41], one could control the angles ( $\gamma, \alpha$ ) of the incident beam, and the excitation energy  $\epsilon$  can be controlled by the junction bias voltage. Then, by mapping out the signal dependence on ( $\gamma, \alpha, \epsilon$ ), one can extract the features of the shifts and, in principle, characterize the gap structure for unconventional superconductors.

Here it should be noted that: While for chiral pairings, the voltage signal is solely due to the shifts in the Andreev reflection, for nonchiral pairings (like the  $d_{x^2-y^2}$ -wave), the signal may have contributions from both normal and Andreev reflections. Since  $\ell_T^e \approx \ell_T^h$ , the net result depends on the probabilities ( $|r_h|^2$  vs  $|r_e|^2$ ) of the two processes. There could be an interesting competition between the two when tuning the excitation energy. Generally, for  $\epsilon$  close to the superconducting gap,  $|r_h|^2$  would dominate over  $|r_e|^2$  [18], so in this case, the signal would be dominated by the shifts in the Andreev reflection.

We remark that real unconventional superconductor materials could have other complicated features, such as multiple Fermi surfaces, multiple bands with different pairing magnitudes, and possible surface (interface) bound states [17,22,42–44]. How these features would affect the anomalous shifts are interesting questions to explore in future studies. Nevertheless, our analysis suggests that a nonzero shift (hence the resulting voltage) is generally expected, owing to the coupling between the Nambu pseudospin and the orbital motion as generated by the

unconventional pair potential. Although its detailed profile requires more accurate material-specific modeling, the key features for the shift, like the period in  $\alpha$  and the gap dependence as listed in Table I, should be robust, since they are determined by the overall characteristic associated with the symmetry of unconventional pairings. This also helps to distinguish the signal from the shift against random noises such as from the impurities or interface roughness. Finally, when the SOC effect is included, it can generate an additional contribution to the shift in the Andreev reflection [16]. However, its dependence on the incident geometry and the excitation energy will be distinct from that due to the unconventional pairings.

The authors thank Fan Yang, Hua Jiang, and D. L. Deng for valuable discussions. This work was supported by the Singapore Ministry of Education AcRF Tier 2 (MOE2017-T2-2-108), the National Key R&D Program of China (2016YFA0300600), and the NSFC (Grant No. 11734003 and 11574029).

- 
- [1] F. Fedorov, Dokl. Akad. Nauk SSSR **105**, 465 (1955).  
 [2] C. Imbert, *Phys. Rev. D* **5**, 787 (1972).  
 [3] M. Onoda, S. Murakami, and N. Nagaosa, *Phys. Rev. Lett.* **93**, 083901 (2004).  
 [4] K. Y. Bliokh and Y. P. Bliokh, *Phys. Rev. Lett.* **96**, 073903 (2006).  
 [5] O. Hosten and P. Kwiat, *Science* **319**, 787 (2008).  
 [6] X. Yin, Z. Ye, J. Rho, Y. Wang, and X. Zhang, *Science* **339**, 1405 (2013).  
 [7] Q.-D. Jiang, H. Jiang, H. Liu, Q.-F. Sun, and X. C. Xie, *Phys. Rev. Lett.* **115**, 156602 (2015).  
 [8] S. A. Yang, H. Pan, and F. Zhang, *Phys. Rev. Lett.* **115**, 156603 (2015).  
 [9] Q.-D. Jiang, H. Jiang, H. Liu, Q.-F. Sun, and X. C. Xie, *Phys. Rev. B* **93**, 195165 (2016).  
 [10] L. Wang and S.-K. Jian, *Phys. Rev. B* **96**, 115448 (2017).  
 [11] K. Y. Bliokh, F. J. Rodriguez-Fortuno, F. Nori, and A. V. Zayats, *Nat. Photonics* **9**, 796 (2015).  
 [12] X. Wan, A. M. Turner, A. Vishwanath, and S. Y. Savrasov, *Phys. Rev. B* **83**, 205101 (2011).  
 [13] S. Murakami, *New J. Phys.* **9**, 356 (2007).  
 [14] A. F. Andreev, *Sov. Phys. JETP* **19**, 1228 (1964).  
 [15] P. G. de Gennes, *Superconductivity in Metals and Alloys* (Benjamin, New York, 1966).  
 [16] Y. Liu, Z.-M. Yu, and S. A. Yang, *Phys. Rev. B* **96**, 121101 (2017).  
 [17] M. Sigrist, A. Avella, and F. Mancini, *AIP Conf. Proc.* **789**, 165 (2005).  
 [18] G. E. Blonder, M. Tinkham, and T. M. Klapwijk, *Phys. Rev. B* **25**, 4515 (1982).  
 [19] S. Kashiwaya and Y. Tanaka, *Rep. Prog. Phys.* **63**, 1641 (2000).  
 [20] See Supplemental Material at <http://link.aps.org/supplemental/10.1103/PhysRevLett.121.176602> for detailed calculations of scattering amplitudes and transverse shift for reflected wave packet, and calculations in the lattice model, which includes Refs. [7,18,19,21–33].  
 [21] C. W. J. Beenakker, R. A. Sepkhanov, A. R. Akhmerov, and J. Tworzydło, *Phys. Rev. Lett.* **102**, 146804 (2009).  
 [22] R. Beiranvand, H. Hamzehpour, and M. Alidoust, *Phys. Rev. B* **94**, 125415 (2016).  
 [23] D. J. BenDaniel and C. B. Duke, *Phys. Rev.* **152**, 683 (1966).  
 [24] Y. Su, H. Liao, and T. Li, *J. Phys. Condens. Matter* **27**, 105702 (2015).  
 [25] T. Ando, *Phys. Rev. B* **44**, 8017 (1991).  
 [26] P. A. Khomyakov, G. Brocks, V. Karpan, M. Zwierzycki, and P. J. Kelly, *Phys. Rev. B* **72**, 035450 (2005).  
 [27] M. Sotoodeh, A. Khalid, and A. Rezazadeh, *J. Appl. Phys.* **87**, 2890 (2000).  
 [28] S. S. Murzin, M. Weiss, A. G. M. Jansen, and K. Eberl, *Phys. Rev. B* **64**, 233309 (2001).  
 [29] Y. Ohno, R. Terauchi, T. Adachi, F. Matsukura, and H. Ohno, *Phys. Rev. Lett.* **83**, 4196 (1999).  
 [30] S. Murakami, N. Nagaosa, and S.-C. Zhang, *Science* **301**, 1348 (2003).  
 [31] N. W. Ashcroft and N. D. Mermin, *Solid State Physics* (Thomson Learning, Boston, 1976).  
 [32] D. Gall, *J. Appl. Phys.* **119**, 085101 (2016).  
 [33] M. Bauer and M. Aeschlimann, *J. Electron Spectrosc. Relat. Phenom.* **124**, 225 (2002).  
 [34] M. J. M. de Jong and C. W. J. Beenakker, *Phys. Rev. Lett.* **74**, 1657 (1995).  
 [35] H. Plehn, U. Günsenheimer, and R. Kümmel, *J. Low Temp. Phys.* **83**, 71 (1991).  
 [36] J. Hara, M. Ashida, and K. Nagai, *Phys. Rev. B* **47**, 11263 (1993).  
 [37] H. Plehn, O.-J. Wacker, and R. Kümmel, *Phys. Rev. B* **49**, 12140 (1994).  
 [38] Y. Tanaka and S. Kashiwaya, *Phys. Rev. Lett.* **74**, 3451 (1995).  
 [39] F. Goos and H. Hänchen, *Ann. Phys. (N. Y.)* **436**, 333 (1947).  
 [40] J. Spector, H. L. Stormer, K. W. Baldwin, L. N. Pfeiffer, and K. W. West, *Appl. Phys. Lett.* **56**, 1290 (1990).  
 [41] D. Dragoman and M. Dragoman, *Prog. Quantum Electron.* **23**, 131 (1999).  
 [42] C. C. Tsuei and J. R. Kirtley, *Rev. Mod. Phys.* **72**, 969 (2000).  
 [43] A. P. Mackenzie and Y. Maeno, *Rev. Mod. Phys.* **75**, 657 (2003).  
 [44] C. Kallin and J. Berlinsky, *Rep. Prog. Phys.* **79**, 054502 (2016).